HHS Public Access

Author manuscript

Kidney Int. Author manuscript; available in PMC 2024 April 01.

Published in final edited form as:

Kidney Int. 2023 October ; 104(4): 740–753. doi:10.1016/j.kint.2023.06.031.

Matrix metalloproteinase-9 regulates afferent arteriolar remodeling and function in hypertension-induced kidney disease

Wenguang Feng[1], **Zhengrong Guan**[1], **Wei-Zhong Ying**[1], **Dongqi Xing**[1], **Kai Er Ying**[1], **Paul W. Sanders**[1,2,3]

[1]Department of Medicine, University of Alabama at Birmingham, Birmingham, Alabama, USA

[2]Department of Cell, Developmental and Integrative Biology, University of Alabama at Birmingham, Birmingham, Alabama, USA

[3]Birmingham Veterans Affairs Health Care System, Birmingham, Alabama, USA

Abstract

This study tested if matrix metalloproteinase (MMP)-9 promoted microvascular pathology that initiates hypertensive (HT) kidney disease in salt-sensitive (SS) Dahl rats. SS rats lacking *Mmp9* ($Mmp9^{-/-}$) and littermate control SS rats were studied after one week on a normotensive 0.3% sodium chloride (Pre-HT SS and Pre-HT $Mmp9^{-/-}$) or a hypertension-inducing diet containing 4.0% sodium chloride (HT SS and HT $Mmp9^{-/-}$). Telemetry-monitored blood pressure of both the HT SS and HT $Mmp9^{-/-}$ rats increased and did not differ. Kidney microvessel transforming growth factor-beta 1 (*Tgfb1*) mRNA did not differ between Pre-HT SS and Pre-HT $Mmp9^{-/-}$ rats, but with hypertension and expression of *Mmp9* and *Tgfb1* increased in HT SS rats, along with phospho-Smad2 labeling of nuclei of vascular smooth muscle cells, and with peri-arteriolar fibronectin deposition. Loss of MMP-9 prevented hypertension-induced phenotypic transformation of microvascular smooth muscle cells and the expected increased microvascular expression of pro-inflammatory molecules. Loss of MMP-9 in vascular smooth muscle cells *in vitro* prevented cyclic strain–induced production of active TGF-β1 and phospho-Smad2/3 stimulation. Afferent arteriolar autoregulation was impaired in HT SS rats but not in HT $Mmp9^{-/-}$ rats or the HT SS rats treated with doxycycline, an MMP inhibitor. HT SS but not HT $Mmp9^{-/-}$ rats showed decreased glomerular Wilms Tumor 1 protein–positive cells (a marker of podocytes) along with increased urinary podocin and nephrin mRNA excretion, all indicative of glomerular damage. Thus, our findings support an active role for MMP-9 in a hypertension-induced kidney microvascular remodeling process that promotes glomerular epithelial cell injury in SS rats.

Correspondence: *Paul W. Sanders, Division of Nephrology, University of Alabama at Birmingham, 1918 University Blvd, MCLM 452, Birmingham, Alabama 35294, USA.* psanders@uab.edu.

AUTHOR CONTRIBUTIONS

WF, ZG, DX, KEY, and WY performed the experiments. WF, ZG, and PWS analyzed the data and interpreted the results of experiments. WF, ZG, and PWS prepared the figures. WF and PWS drafted the manuscript. WF, ZG, and PWS edited and revised the manuscript. WF, ZG, DX, KEY, WY, and PWS approved the final version of the manuscript. WF and PWS conceived and designed the research.

DISCLOSURE

All the authors declared no competing interests.

Keywords

Dahl salt-sensitive rat; hypertension; kidney autoregulation; TGF-β

Hypertension-induced nephropathy is a common cause of chronic kidney disease and is the second leading cause of end-stage kidney disease, producing over a quarter of all cases of end-stage kidney disease in the United States.[1–3] With the high prevalence of hypertension in the population, however, the percentage of hypertensive patients who ultimately develop end-stage kidney disease has been low (0.5%–1% of the hypertensive population),[3] suggesting a predisposition to the development of this form of hypertensive target organ injury. Remodeling of afferent arterioles is a hallmark of human hypertensive nephropathy; accumulation of extracellular matrix and podocyte loss with albuminuria and ultimately glomerulosclerosis and interstitial fibrosis generally accompany the vascular changes.[4,5]

An inherent predisposition to hypertension-induced kidney disease is observed not only in humans but also in rodent models.[6–13] Dahl salt-sensitive (SS) rats are a very well characterized model of hypertension and particularly kidney injury.[14–16] SS rats uniformly develop hypertension followed by proteinuria and progressive loss of kidney function.[15,17] Glomerular injury results from a vascular disease process that resembles the human condition of hypertension-induced microvascular remodeling in the kidney.[15,17] Studies of SS rats support the concept that the remodeling process was related to an intrinsic disorder of vascular smooth muscle cells (VSMCs).[16,18] Miller *et al.*[19] strengthened this observation by showing that knocking out the gene that encodes the SH2 adaptor protein p66Shc prevented cell signaling responses of VSMCs to hypertension and protected the genetically modified SS rats from hypertension-induced nephropathy.

Matrix metalloproteinase-9 (MMP-9) participates in the pathophysiology of chronic kidney disease,[20] but mechanisms of injury are incompletely understood. MMP-9 activity, but not the activity of the other gelatinase MMP-2, associates with albuminuria in patients and in the Munich Wistar Frömter rat, a model of progressive proteinuria.[21] Williams *et al.*[22] used 2 different nonselective metalloprotease inhibitors to show an improvement in glomerulosclerosis and interstitial fibrosis without reducing blood pressure in SS rats. Avian erythroblastosis virus E26 oncogene homolog-1 is a transcription factor that is involved in the regulation of the renovascular response to hypertension in SS rats.[18,23,24] Importantly, MMP-9 is a downstream target of E26 oncogene homolog-1.[25] A unique model of SS rats that lack *Mmp9* (termed $SS^{Mmp9-/-}$) was therefore generated to test the hypothesis that MMP-9 promoted critical microvascular remodeling and hypertension-induced kidney injury. The findings of the present studies supported an important role of MMP-9 in kidney microvascular pathobiology and end-organ kidney damage in hypertension.

METHODS

Animals

Studies were conducted using Dahl salt-sensitive rats (SS/JrHsd/Mcw, abbreviated as SS, rats)[10,26–28] and Dahl SS/JrHsd/Mcw rats that have a deletion mutation in *Mmp9* (SS$^{Mmp9-/-}$ rats). The original SS and SS$^{Mmp9-/-}$ strains of rats were generous gifts from Dr. Aron Geurts, Medical College of Wisconsin. SS$^{Mmp9-/-}$ rats were genetically identical to littermate SS rats, except for homozygous mutation of *Mmp9*, introduced using genome engineering with the CRISPR/Cas9 system, which targeted exon 4 of the rat *Mmp9* gene and resulting in a frameshift mutation, confirmed by genotyping with TaqMan probe real-time polymerase chain reaction (PCR; Transnetyx; Figure 1). Littermate SS rats served as controls in these experiments. Rat breeders and weanlings were fed a purified rodent diet containing 0.3% NaCl (Dyet#100077, AIN-76A Purified Rodent Diet with 0.3% NaCl, Dyets Inc.) and tap water *ad libitum* until study. In some experiments, doxycycline (Dox, D9891, MilliporeSigma), 30 mg/kg/d, in drinking water was given to SS rats 3 days before the termination of the study.

Genotyping and confirmation of *Mmp9* mutation

For genotyping, TaqMan probes that recognized the 8-bp deletion sequence (mutant probe) or wild-type sequence (wild-type probe) were designed. The wild-type TaqMan probe was 5′- ACGGG-TATCCCTTCGACG-3′, and the TaqMan probe to detect the mutation in *Mmp9* was 5′-CCCCGGGTATCGAC-3′. The genotypes were determined as wild-type (homozygous SS) or homozygous SS$^{Mmp9-/-}$ for the mutation, depending on whether the samples were positive with only wild-type probes or positive with only mutant probes, respectively, as previously described.[24] DNA samples of rats in the study were amplified with real-time PCR and used to determine genotype (Transnetyx). The forward primer sequence was CCGCCTCTGCAGAGCA, and the reverse sequence was GTGTGCCAGTAGACCATCCTT.

Experiments were performed using 9- to 12-week-old age-matched male SS$^{Mmp9-/-}$ rats and littermates (SS). Male rats were used in these studies, because female SS rats may have different pathogenetic processes that generate and modify hypertension and end-organ injury.[29] Because of the need to monitor blood pressure in awake unrestrained animals, continuous monitoring of blood pressure was performed using radiotelemetry.[30,31] Rats were anesthetized using 2% isoflurane, and an implantable radiotelemetry transmitter (HD-S10, Data Sciences International [DSI]) was inserted into the left femoral artery to continuously record awake unrestrained blood pressure.[32] Rats were allowed 7 days to recover and were then divided into 4 groups (n = 6–9 rats per group) and fed either a control diet containing 0.3% NaCl (AIN-76A Purified Rodent Diet with 0.3% NaCl, Dyets Inc.; groups termed Pre-HT SS and Pre-HT SS$^{Mmp9-/-}$) or a 4% NaCl diet for 1 week (Dyet#113756, AIN-76A Purified Rodent Diet with 4.0% NaCl, Dyets Inc.) to induce hypertension (groups termed HT SS and HT SS$^{Mmp9-/-}$). Blood pressure was continuously monitored in awake unrestrained rats throughout the 7-day study.

On day 6 of high-salt feeding, some rats of the 4 experimental groups were placed in metabolic cages for 24 hours to collect urine to determine concentrations of albumin and creatinine. Urinary albumin concentrations were determined by enzyme-linked immunosorbent assay (catalog no. E110–125, Bethyl) and normalized against urinary creatinine concentration (catalog no. DICT-500, Bioassay Systems). Rats were anesthetized; blood was collected for determination of serum creatinine using liquid chromatography–tandem mass spectrometry (Agilent 6460 C triple quad tandem mass spectrometry system)[33]; and the kidneys were harvested for physiology, histology, and molecular analyses.

Western blot analysis

Kidney tissues were homogenized and sonicated in Pierce RIPA Buffer (Catalog No. 89901, Thermo Scientific) with Halt Protease and Phosphatase Inhibitor Cocktail (Catalog No. 1861284, Thermo Scientific). The total soluble protein concentration in lysates was determined using a bicinchoninic acid assay kit (catalog no. 23227, BCA Protein Assay Reagent Kit, Thermo Scientific). Samples were boiled for 3 minutes in Laemmli buffer and separated using 7% to 12% sodium dodecylsulfate–polyacrylamide gel electrophoresis (catalog no. 5671044 Bio-Rad Laboratories) before electrophoretic transfer onto polyvinylidene diflouride membranes. The membranes were blocked in 5% nonfat milk and then probed with an MMP-9 antibody (catalog no. ab76003, Abcam; or catalog no. sc13520, MMP-9 antibody [7–11C], Santa Cruz Biotechnology, Inc.; diluted 1:1000). After washes, the blots were incubated for 1 hour at room temperature with Alexa Fluor 680 or 790 conjugated AffiniPure anti-rabbit secondary antibody (1:10,000 dilution). The bands were detected using the Odyssey CLx Infrared Imaging System (LI-COR Biosciences), and densitometric analysis was performed using Image Studio Software (LI-COR Biosciences).

In vitro blood-perfused juxtamedullary nephron preparation

Autoregulatory behavior of afferent arterioles was assessed in experimental groups of animals by using the *in vitro* blood-perfused juxtamedullary nephron technique, as described previously.[34–36] In the first experiment, 4 groups of rats were included: Pre-HT SS, Pre-HT SS$^{Mmp9-/-}$, HT SS, and HT SS$^{Mmp9-/-}$ (n = 5–7 rats examined per group). In a second experiment, we used the MMP inhibitor Dox (D9891), 30 mg/kg/d, in drinking water[37,38] to assess the effect of MMP-9 on autoregulation. Additional 2 groups of rats were included: Pre-HT SS + Dox and HT SS þ Dox. Briefly, 2 identical rats were anesthetized with thiobutabarbital i.p. (100 mg/kg body weight) for each juxtamedullary nephron experiment. The right kidney was cannulated and continuously perfused over the course of the kidney dissection with ~200 to 300 ml of Tyrode's buffer (Sigma-Aldrich) containing 5.2% bovine serum albumin (Calbiochem). Perfusate blood was collected via a carotid artery cannula from the kidney donor and an identical blood donor and centrifuged to obtain the plasma and erythrocytes for kidney perfusion (hematocrit of ~33%). The inner cortical surface of the right kidney was exposed, and the ends of the intrarenal arteries and arterial branches were tied with a 10–0 nylon suture to restore kidney perfusion pressure. After completion of the dissection, the kidney was switched to the reconstituted blood at a perfusion pressure of 100 mm Hg. The image of the kidney was displayed on a video monitor via a high-resolution NC-70 Newvicon video camera (Dage-MTI) and recorded on digital video disk for later

analysis. After at least 20-minute equilibration period, afferent arteriolar autoregulatory responses were assessed as perfusion pressure was reduced from 100 to 65 mm Hg and then increased to 170 mm Hg in 15-mm Hg increments at 5-minute intervals. The inner arteriole diameter was measured every 12 seconds at a single site using a calibrated image-shearing monitor (model 908, Vista Electronics) and was calculated from the average of all diameter measurements collected during the final 2 minutes of each treatment period.

Kidney microvessel isolation for mRNA expression analysis

Briefly, rats were anesthetized with thiobutabarbital for retrograde perfusion through the abdominal aorta. The kidneys were perfused with 5 to 10 ml of Tyrode's buffer to flush out the blood and placed in ice-cold physiological salt solution. Medulla and intrarenal arteries were removed, and cortical tissue was gently pressed through a nylon membrane sieve (100 μm pore size, BioDesign, Inc.). The kidney tissue was transferred into RNA*later* stabilization solution (Invitrogen, Thermo Fisher Scientific). Segments of arcuate and interlobular arteries with attached afferent arterioles were identified and collected by microdissection under a stereoscope for mRNA extraction.

Real-time quantitative reverse transcription PCR analysis of gene expression in samples of kidney microvessels and urine

Kidney microvascular RNA was extracted from dissected kidney microvessels with TRIzol (Invitrogen). Urinary RNA was isolated from 24-hour urinary samples with a kit (Zymo Research). Samples were treated with DNAase I to remove genomic DNA. Protein- and DNA-free RNA was reverse transcribed to cDNA with use of SuperScript IV (Invitrogen). cDNA was amplified by PCR in the LightCycler 480 System (Roche) for 40 cycles using the SYBR Green method (Applied Biosystems) and specific primers (Table 1); relative RNA levels were calculated with the PCR threshold cycle software and a standard equation (Applied Biosystems). mRNA expression was normalized against glyceraldehyde-3-phosphate dehydrogenase (GAPDH) for each sample and then standardized to the group of Pre-HT SS as 1.

Immunohistochemical and immunofluorescence staining

Three-micrometer-thick kidney sections were prepared from paraffin-embedded tissues. After deparaffinization, antigen retrieval was performed with Antigen Unmasking Solution (H-3300, Vector Laboratories).

For immunohistochemical staining, an avidin-biotin-peroxidase complex-based immunohistochemical technique was used to detect Wilms' tumor 1 (WT1) protein, a podocyte marker, in glomeruli. Section peroxidase activity was quenched with BLOXALL Endogenous Blocking Solution (SP-6000, Vector Laboratories); endogenous biotin was blocked with the Avidin/Biotin Blocking Kit (SP-2001, Vector Laboratories); and other nonspecific staining was blocked with normal serum. Sections were incubated with the primary antibody rabbit antibody against WT1 (ab224806, Abcam) overnight, followed by application of a biotinylated goat anti-rabbit antibody for 30 minutes. Slides were then incubated with VEC-TASTAIN ABC Kit (PK-4001, Vector Laboratories) reagents according to the manufacturer's instructions and developed with Vector NovaRED Substrate Kit

(SK-4800, Vector Laboratories) substrate. Images were acquired using a Leica DM6000 microscope (Leica Microsystems). WT1-positive cells were counted in at least 30 glomeruli in each section of the experimental groups by a blinded observer. Counts were normalized using the glomerular area determined by Image J (National Institutes of Health) and then averaged per kidney. Values were averaged in experimental groups and expressed as mean ± SEM.

For immunofluorescence staining, sections were incubated with rabbit primary antibodies to phosphorylated Smad2 (#18338, Cell Signaling) and fibronectin (ab2413, Abcam) at 4 °C overnight. Another primary antibody to smooth muscle actin (Mouse, 1A4, Invitrogen; or Rabbit, ab5694, Abcam) was also used to outline the vessel in kidney sections. Sections were washed and incubated with the respective secondary antibodies conjugated with either Alexa Fluor 488 (green, Invitrogen) or Alexa Fluor 594 (red, Invitrogen). Counterstaining of the nucleus was achieved by mounting sections with hardset mounting media containing 4′,6-diamidino-2-phenylindole (DAPI, blue color; Vector Laboratories). Negative controls by omission of the primary antibody were included in each experiment. Images were acquired using a Leica DM6000 epifluorescence microscope (Leica Microsystems) with a Hamamatsu ORCA ER cooled CCD camera (Hamamatsu Photonics) and SimplePCI software (Compix Inc).

Producing cyclic strain in primary cultures of VSMCs

Primary cultures of VSMCs were derived from 10-week-old inbred SS or SS$^{Mmp9-/-}$ rats. Thoracic aortas were obtained by careful dissection under anesthesia. The adventitia and endothelium were carefully removed from segments of aorta and washed several times with Dulbecco's modified Eagle's medium (Gibco, Thermo Fisher Scientific). The segments were cut into ~0.5-mm squares, placed on 25-mm Petri dishes, cultured in Dulbecco's modified Eagle's medium containing 10% fetal bovine serum at 37 °C and 5% CO_2. The cells that grew from the explants had become relatively confluent within a period of ~2 to 3 weeks, as previously described.[39,40] They were then rinsed with phosphate-buffered saline and subsequently passaged with trypsin. The resulting suspension of cells in Dulbecco's modified Eagle's medium supplemented with 10% fetal bovine serum was pipetted into the flask and placed back in the incubator. The medium was changed the next day to remove trypsin and cell debris. VSMCs in the first or second passage were stored in liquid nitrogen until use.[40]

To generate cyclic strain, cells were cultured in Dulbecco's modified Eagle's medium supplemented with 10% fetal bovine serum, 4 mmol/l of l-glutamine, 100 U/ml of penicillin, and 100 μg/ml of streptomycin. Cells were identified as smooth muscle cells by their characteristic morphology and positive immunostaining for α-smooth muscle actin (clone 1A4, Dako). All experiments were performed using VSMCs in the early (<5) passage. VSMCs were seeded onto 6-well BioFlex plates coated with collagen type IV (FlexCell) and grown to 80% confluence and were serum starved for 12 hours before the study.[40] Biaxial cyclic stretch was performed using the FlexCell 6000 Strain Unit (FlexCell International Corporation). Cells were stretched for using a standardized regimen (8 hours, 15% elongation, 1 Hz frequency) in accordance with a previous study[41] and our preliminary

studies. At the end of the experiment, cells were harvested from mRNA and protein analyses and medium was harvested to determine active transforming growth factor β1 (TGF-β1) using a kit (DB100C, Human/Mouse/Rat/Porcine/Canine TGF-β1 ImmunoAssay Quantikine ELISA kit, Promega).

Statistical analyses

Data are expressed as mean ± SEM. Data from determination of blood pressure using telemetry and from autoregulation experiments were analyzed using 2-way analysis of variance for repeated measures. All other data were analyzed using 2-way analysis of variance. When the overall F test result of analysis of variance was significant, a Dunnett or Turkey *post hoc* test was also performed. A P value of <0.05 assigned statistical significance.

Study approval

This study was performed in accordance with the recommendations in the National Institutes of Health's *Guide for the Care and Use of Laboratory Animals*. The Institutional Animal Care and Use Committee at the University of Alabama at Birmingham approved the project.

RESULTS

Characterization of SS$^{Mmp9-/-}$ rats

The CRISPR/Cas9 system was used to delete 1-bp (t) and insert 5-bp (cgggta) in exon 4 of the *Mmp9* gene, producing a frameshift mutation in exon 4 (Figure 1a), and a premature stop codon in exon 8. Homozygous SS$^{Mmp9-/-}$ and littermate control SS rats were confirmed using TaqMan probe real-time PCR (Transnetyx; Figure 1b) and were bred in the Animal Resources Program Facility at the University of Alabama at Birmingham. Littermate SS control and SS$^{Mmp9-/-}$ rats were maintained on the 0.3% NaCl diet and then switched to the 4% NaCl diet for 1 week to induce hypertension. Western analysis at day 7 confirmed the absence of MMP-9 in SS$^{Mmp9-/-}$ rats on both diets and demonstrated that expression of MMP-9 relative to glyceraldehyde-3-phosphate dehydrogenase in the kidney cortex increased in HT SS compared with Pre-HT SS rats (Figure 1c; Supplementary Figure S1).

At day 7, total RNA was extracted from dissected kidney microvessels. Relative expression of *Mmp9* determined using the SYBR Green reverse transcription PCR method and primers listed in Table 1 showed lower levels of *Mmp9* mRNA in both Pre-HTor HT SS$^{Mmp9-/-}$ rats than in Pre-HTor HT SS control rats. Development of hypertension increased *Mmp9* mRNA expression by 1-fold in kidney microvessels of HT SS rats (Pre-HT SS vs. HT SS, 1.03 ± 0.08 vs. 1.99 ± 0.2; $P < 0.05$).

Kidney injury was detected in HT SS rats but was abrogated in HT SS$^{Mmp9-/-}$ rats despite radiotelemetry-monitored blood pressure that did not differ

At baseline, systolic blood pressure and diastolic blood pressure did not differ between SS and SS$^{Mmp9-/-}$ rats. One week on the 4% NaCl diet increased both daytime and nighttime systolic blood pressure and diastolic blood pressure in SS and SS$^{Mmp9-/-}$ rats to levels that

did not differ between the groups (n = 6 rats in each group; P > 0.05; Figure 2a). Heart rates also did not differ between SS and SS$^{Mmp9-/-}$ rats (Supplementary Figure S2).

Assessment of serum creatinine concentration and urinary albumin excretion rate revealed that kidney injury was present in HT SS rats but was prevented in HT SS$^{Mmp9-/-}$ rats despite a similar increase in blood pressure. Although mean serum creatinine concentration and mean urinary albumin excretion rate did not differ between Pre-HT SS and Pre-HT SS$^{Mmp9-/-}$ rats maintained on the 0.3% NaCl diet, after 1 week of high salt intake, mean serum creatinine concentration and 24-hour urinary albumin excretion rate increased in HT SS rats and were higher than mean values observed in HTSS$^{Mmp9-/-}$ rats (n = 6–9 rats in each group; P < 0.05; Figure 2b and c).

Podocyte injury increased in HT SS but not in SS$^{Mmp9-/-}$ rats

Because of the early development of albuminuria, at day 7 podocyte damage was examined by quantifying WT1-positive podocytes in glomeruli and podocin and nephrin mRNA in urine. Blind analysis of photomicrographs of immunohistochemical staining using WT1 antibody to outline the nuclei of podocytes showed that HT decreased WT1-positive cells in HT SS but not in HT SS$^{Mmp9-/-}$ rats (n = 6 rats in each group; HT SS vs. HT SS$^{Mmp9-/-}$, 3.66 ± 0.97 vs. 9.29 ± 0.91; P < 0.05; Figure 3a). At day 7, HT SS rats showed an increase (P < 0.05 vs. Pre-HT SS) in mean urinary podocin and nephrin mRNA excretion compared with Pre-HT SS rats. Compared with HT SS rats, urinary excretion of podocin and nephrin in HT SS$^{Mmp9-/-}$ rats was less (n = 6 rats in each group; P < 0.05; HT SS vs. HT SS$^{Mmp9-/-}$, podocin: 18.9 ± 4.18 vs. 8.23 ± 1.55; nephrin: 16.0 ± 3.15 vs. 9.25 ± 2.27; Figure 3b and c).

Kidney autoregulation was preserved in HT SS$^{Mmp9-/-}$ and HT SS rats treated with the MMP inhibitor

Mean diameters of afferent arterioles at baseline did not differ among experimental groups of rats (P > 0.05; Figure 4; Supplementary Table S1). Similarly, the vasoconstrictor responses of afferent arterioles to KCl (55 mM) did not differ among the 6 groups under study (Supplementary Figure S3). Afferent arterioles from Pre-HT SS and Pre-HT SS$^{Mmp9-/-}$ rats exhibited normal autoregulatory behavior. Decreasing kidney perfusion pressure from 100 to 65 mm Hg increased the afferent arteriolar diameter to 115% ± 3% and 114% ± 3% of baseline diameter (P < 0.05; Figure 4a), respectively. Stepwise increases in perfusion pressure to 170 mm Hg decreased arteriolar diameter to 76% ± 4% and 76% ± 2% of baseline diameter (P < 0.05), respectively. In contrast, pressure-mediated afferent arteriolar responses were markedly impaired in HT SS rats. Baseline diameter averaged 14.3 ± 1.3 μm and remained between 107% ± 2% and 102% ± 3% (P < 0.05 vs. Pre-HT SS) of baseline diameter over the 65 to 170 mm Hg pressure range tested (Figure 4). Importantly, kidney autoregulation remained intact in HT SS$^{Mmp9-/-}$ rats. Baseline diameter averaged 13.5 0.7 mm in HT SS$^{Mmp9-/-}$ rats. Decreasing kidney perfusion pressure from 100 to 65 mm Hg resulted in a diameter increase to 113% ± 3% of baseline in the HT + Dox group, whereas increasing perfusion pressure to 170 mm Hg resulted in a pressure-dependent vasoconstriction to 71% ± 5% (P < 0.05 vs. HT SS). Like HT SS$^{Mmp9-/-}$ rats, kidney autoregulation was also preserved in SS rats treated with Dox (HT SS + Dox

rats; Figure 4b). One week on the 4% NaCl diet increased both daytime and nighttime systolic blood pressure and diastolic blood pressure in groups of SS rats and SS rats on Dox treatment to levels that did not differ ($P > 0.05$) between the HT SS and HT + Dox groups (Supplementary Figure S4). Dox treatment alone did not alter the autoregulatory profile in pre-HT rats. Baseline diameter averaged 12.9 ± 0.5 μm in HT SS + Dox rats. Decreasing kidney perfusion pressure from 100 to 65 mm Hg resulted in a diameter increase to 113% ± 3% of baseline, whereas increasing perfusion pressure to 170 mm Hg resulted in a pressure-dependent vasoconstriction to 77% ± 1% ($P < 0.05$ vs. HT SS).

TGF-β pathway was activated and fibronectin increased in the kidney microvasculature in HT SS but not in SS$^{Mmp9-/-}$ rats

At day 7, immunofluorescence microscopy using α-smooth muscle actin antibody (green) to outline the arteriole showed the appearance of MMP-9 and activation of Smad2 in the smooth muscle layer of kidney microvessels of HT SS rats as well as production of fibronectin in and around arterioles (Figure 5; Supplementary Figure S5).

Real-time quantitative reverse transcription PCR using total RNA extracted from dissected kidney microvessels at day 7 showed that basal mRNA levels of *Mmp9*, *Tgfb1*, and *Fn1* were low in Pre-HT SS and Pre-HT SS$^{Mmp9-/-}$ rats and were significantly increased in HT SS rats but not in microvessels of HT SS$^{Mmp9-/-}$ rats ($n = 6$ animals in each group; HT SS vs. Pre-HT SS, Pre-HT SS$^{Mmp9-/-}$, or HT SS$^{Mmp9-/-}$ groups; $P < 0.05$; Figure 5).

Expression of pro-inflammatory and pro-osteogenic molecules increased in the kidney microvasculature in HT SS but not in SS$^{Mmp9-/-}$ rats

Along with activation of the TGF-β pathway, we determined relative mRNA expression of several additional molecules known to affect vascular function through inflammation and calcification. Relative microvascular mRNA expression of P-selectin, Toll-like receptor 2, and intercellular adhesion molecule increased 5.0-, 2.2-, and 1.8-fold, respectively, in HT SS rats but did not change in HT SS$^{Mmp9-/-}$ rats (Figure 6). Similarly, relative microvascular mRNA expression of Runt-related transcription factor 2, also known as core binding factor subunit alpha 1, periostin, and osteopontin increased 1.6-, 4.2-, and 3.8-fold, respectively, in HT SS rats but did not increase in HT SS$^{Mmp9-/-}$ rats ($n = 6$ rats in each group; $P < 0.05$ vs. HT SS$^{Mmp9-/-}$; Figure 6).

Producing cyclic strain in cultures of VSMCs from SS but not from SS$^{Mmp9-/-}$ rats produced active TGF-β and activated the canonical TGF-β pathway

To provide additional mechanistic insight, primary cultures of VSMCs from SS and SS$^{Mmp9-/-}$ rats were subjected to cyclic strain. Under static conditions, expression of *Tgfb*, amount of active TGF-β1 in the medium, and activation of the Smad-signaling pathway were low and did not differ between VSMCs from either strain of rats. Cyclic strain (15% elongation at 1 Hz) generated increases in mRNA of TGF-β, amount of TGF-β1 in the medium, and activation of Smad signaling in VSMCs from SS rats but not VSMCs from SS$^{Mmp9-/-}$ rats (Figure 7).

DISCUSSION

Hypertension-induced nephropathy and hypertension *per se* may be inherited as separate genetic traits in SS rats.[42] These conditions, however, are usually interrelated as progression of albuminuria and deterioration in kidney function in these animals is dependent on the development of hypertension.[15] The present series of experiments examined alterations in kidney microvascular function during hypertension-induced kidney disease in SS rats. New findings included the following: (i) loss of *Mmp9* did not alter the sustained increase in telemetry-monitored blood pressure in SS$^{Mmp9-/-}$ rats over the study period, but did prevent the attendant increase in serum creatinine and albuminuria; (ii) HT SS but not HT SS$^{Mmp9-/-}$ rats demonstrated the loss of afferent arteriolar autoregulatory capability known to occur with hypertension in this rodent strain[43,44]; (iii) loss of *Mmp9* inhibited activation of TGF-β1 in kidney arterioles *in vivo* and cultured VSMCs *in vitro*; (iv) loss of *Mmp9* prevented hypertension-associated increases in kidney microvascular expression of Runt-related transcription factor 2 (core binding factor subunit alpha 1), a transcription factor that serves as an essential and sufficient initiator of osteoblast differentiation,[45–48] and regulates transcription of bone matrix protein genes that include periostin and osteopontin,[49,50] which were increased 4.2- and 3.3-fold, respectively, in HT SS rats; and (v) HT SS but not HT SS$^{Mmp9-/-}$ rats showed loss of glomerular WT1-positive cells and increases in urinary podocin and nephrin mRNA. These studies discovered in SS rats a *Mmp9*-dependent, hypertension-induced osteogenic phenotypic switch by VSMCs, with concomitant dysregulation of microvascular function. The loss of *Mmp9* provided a renoprotective role that limited the development of hypertension-induced nephropathy.

By preventing the transmission of increased arterial pressure into glomerular capillaries, the afferent arteriole is perhaps the most important vessel responsible for renoprotection in hypertension.[51–55] Some hypertensive patients demonstrate glomerular hyperfiltration and absent autoregulation of glomerular filtration rate; this population also experienced a 5-fold increased incidence of hypertension-mediated end-stage kidney disease.[56] Prehypertensive SS rats do not manifest glomerular hypertension,[57] but develop severely impaired autoregulation with sustained hypertension.[18,44,58] Autoregulation is a function of the arteriolar myogenic response and tubuloglomerular feedback (TGF).[8,59–61] Impaired autoregulation from altered myogenic responses has been demonstrated in SS rats,[44] but TGF responses are preserved in this model.[62] It is possible that the lack of *Mmp9* may have enhanced TGF and restored afferent arteriolar autoregulation, which include both myogenic and TGF responses in the *in vitro* blood perfused juxtamedullary nephron preparation.[63] Although the present study did not directly examine TGF in this model, the middle segment rather than the distal segment of the afferent arteriole was examined in this study. This approach limited the effect of TGF, permitting the myogenic response to become the major component of the overall autoregulatory response.[64] Along with evidence of arteriolar remodeling, the present study showed that hypertension-induced impairment of autoregulation of the afferent arteriole was prevented in SS$^{Mmp9-/-}$ rats. In animal models[65] as well as humans,[66] podocyte loss is associated with albuminuria and progressive chronic kidney disease with glomerulosclerosis and interstitial fibrosis. In this study, podocyte loss and increased urinary podocin and nephrin mRNA correlated with impaired autoregulation

of the afferent arteriole in HT SS rats. These findings are consistent with barotrauma-induced podocyte detachment, which occurs in the presence of augmented mechanical distention and shear forces.[67] The demonstrated prevention of arteriolar remodeling and preservation of afferent arteriolar autoregulation along with prevention of podocyte injury in HT SS$^{Mmp9-/-}$ rats supported a critical role of expression of MMP-9 in afferent arteriolar function and attendant glomerular injury during systemic hypertension in this model.

The case for altered activity of MMP-9 in kidney diseases has been considered in several studies, but the findings are complicated and occasionally contradictory.[68] MMP-9 is considered renoprotective in acute kidney injury, because mice lacking *Mmp9*, for example, demonstrate more severe injury, likely because of increased apoptosis in the tubular nephron from disruption of the stem cell factor pathway.[69] Other investigators showed that loss of *Mmp9* was not protective in acute kidney injury after bilateral kidney pedicle clamping, but limited microvasular rarefaction in their mouse model.[70] Further, reductions in MMP-9 levels with diminished degradation of extracellular matrix proteins have been correlated with the development of glomerulosclerosis and tubulointerstitial fibrosis in other rodent models of chronic kidney disease.[71] In contrast to these findings, removal of MMP-9 prevented changes in afferent arteriolar function and attendant glomerular epithelial cell injury.

The underlying mechanism by which removal of MMP-9 improved renovascular function in this model is supported by *in vivo* and *in vitro* studies. Although substrates for MMP-9 are classically matrix proteins, MMP-9 also cleaves latent TGF-β, releasing the active form of the molecule.[72] The studies showed activation of the canonical TGF-β pathway in the arterioles of HT SS rats but did not develop in HT SS$^{Mmp9-/-}$ rats. Levels of active TGF-β in the medium and phosphorylated Smad2/3 increased when cyclic strain was applied to cultured VSMCs from SS but not VSMC from SS$^{Mmp9-/-}$ rats, indicating that MMP-9 from VSMCs was sufficient to activate the canonical TGF-β pathway in these cells. The addition of recombinant active TGF-β can acutely impair autoregulation.[73] In response to various environmental stresses, however, VSMCs are known to undergo phenotypic transformation from a contractile to a synthetic phenotype.[74] TGF-β also promotes osteoblastic transformation of VSMCs by increasing Runt-related transcription factor 2 through the Smad-signaling pathway.[75] The findings of the present study—increased TGF-β, Smad signaling, fibronectin, Runt-related transcription factor 2, and osteopontin—supported this function of MMP-9 in the microvascular remodeling process that developed during hypertension in SS but not in SS$^{Mmp9-/-}$ rats.

In summary, the combined findings of the present study uncover an active role of VSMC-derived MMP-9 in a hypertension-induced kidney microvascular remodeling process that promoted glomerular epithelial cell injury in SS rats. Although MMP-9 is involved in kidney microvascular structure and function, a concomitant intrinsic role of MMP-9 in the glomerular pathology cannot be excluded. Future studies are also required to determine whether other cellular sources participate, such as macrophages that infiltrate around the vascular wall during the remodeling process.[18] Although these findings explain hypertension-induced nephropathy in SS rats, a renovascular role of *Mmp9* in other animal models and in human hypertensive nephrosclerosis remains to be determined. Dox did not reduce the growth rate of small abdominal aortic aneurysms in patients, but the

findings demonstrated the feasibility of treatment for 2 years with minimal adverse drug effects.[76] The use of Dox or other MMP-9 inhibitor in doses that preserve afferent arteriolar autoregulation raises the exciting potential that these pharmaceutical agents may mitigate hypertension-induced kidney injury in susceptible populations.

Supplementary Material

Refer to Web version on PubMed Central for supplementary material.

ACKNOWLEDGMENTS

We thank Aron Geurts of Medical College of Wisconsin for salt-sensitive rats that lack matrix metalloproteinase-9 (*Mmp9*). We thank the University of Alabama at Birmingham–University of California San Diego O'Brien Center for Acute Kidney Injury Research for creatinine measurements and the Heflin Center for Genomic Sciences at UAB for the use of Roche LightCycler 480 384-well real-time polymerase chain reaction.

This work was supported in part by an American Heart Association Scientist Development Grant (15SDG25760063), a Merit Award (1 I01 BX005640) from the U.S. Department of Veterans Affairs Basic Sciences R&D (BSRD) Service, a National Institutes of Health George M. O'Brien Kidney and Urological Research Centers Program (P30 DK079337), NIH R56 HL128285 (to DX), NIH R01 DK106500 (to ZG), a UAB Anderson Innovation Award, and a UAB School of Medicine AMC21 Multi-PI Grant.

REFERENCES

1. Centers for Disease Control and Prevention. Health, United States: 2011: Table 51. End-stage renal disease patients, by selected characteristics: United States, selected years 1980–2010. Accessed September 25, 2019. cdc.gov/nchs/data/hus/2011/051.pdf
2. Ozieh MN, Gebregziabher M, Ward RC, et al. Creating a 13-year national longitudinal cohort of Veterans with chronic kidney disease. BMC Nephrol. 2019;20:241. [PubMed: 31269903]
3. United States Renal Data System. 2019 USRDS Annual Data Report: Epidemiology of Kidney Disease in the United States. National Institutes of Health, National Institute of Diabetes and Digestive and Kidney Diseases; 2019.
4. Seccia TM, Caroccia B, Calo LA. Hypertensive nephropathy: moving from classic to emerging pathogenetic mechanisms. J Hypertens. 2017;35:205–212. [PubMed: 27782909]
5. Fogo A, Breyer JA, Smith MC, et al. AASK Pilot Study Investigators. Accuracy of the diagnosis of hypertensive nephrosclerosis in African Americans: a report from the African American Study of Kidney Disease (AASK) trial. Kidney Int. 1997;51:244–252. [PubMed: 8995739]
6. Kottgen A, Pattaro C, Boger CA, et al. New loci associated with kidney function and chronic kidney disease. Nat Genet. 2010;42:376–384. [PubMed: 20383146]
7. Pattaro C, Kottgen A, Teumer A, et al. Genome-wide association and functional follow-up reveals new loci for kidney function. PLoS Genet. 2012;8:e1002584. [PubMed: 22479191]
8. Liu CT, Garnaas MK, Tin A, et al. Genetic association for renal traits among participants of African ancestry reveals new loci for renal function. PLoS Genet. 2011;7:e1002264. [PubMed: 21931561]
9. Okada Y, Sim X, Go MJ, et al. Meta-analysis identifies multiple loci associated with kidney function-related traits in east Asian populations. Nat Genet. 2012;44:904–909. [PubMed: 22797727]
10. Dahl LK, Heine M, Tassinari L. Effects of chronic excess salt ingestion: evidence that genetic factors play an important role in susceptibility to experimental hypertension. J Exp Med. 1962;115:1173–1190. [PubMed: 13883089]
11. Ying W-Z, Xia H, Sanders PW. Nitric oxide synthase (NOS2) mutation in Dahl/Rapp rats decreases enzyme stability. Circ Res. 2001;89:317–322. [PubMed: 11509447]
12. Ying WZ, Sanders PW. Dietary salt enhances glomerular endothelial nitric oxide synthase through TGF-β1. Am J Physiol. 1998;275:F18–F24. [PubMed: 9689000]

13. Garrett MR, Joe B, Yerga-Woolwine S. Genetic linkage of urinary albumin excretion in Dahl salt-sensitive rats: influence of dietary salt and confirmation using congenic strains. Physiol Genomics. 2006;25:39–49. [PubMed: 16534143]
14. Chen PY, Sanders PW. l-Arginine abrogates salt-sensitive hypertension in Dahl/Rapp rats. J Clin Invest. 1991;88:1559–1567. [PubMed: 1658045]
15. Chen PY, St. John PL, Kirk KA, et al. Hypertensive nephrosclerosis in the Dahl/Rapp rat: initial sites of injury and effect of dietary l-arginine administration. Lab Invest. 1993;68:174–184. [PubMed: 8441251]
16. Wang PX, Sanders PW. Mechanism of hypertensive nephropathy in the Dahl/Rapp rat: a primary disorder of vascular smooth muscle. Am J Physiol Renal Physiol. 2005;288:F236–F242. [PubMed: 15583217]
17. Chen PY, Sanders PW. Role of nitric oxide synthesis in salt-sensitive hypertension in Dahl/Rapp rats. Hypertension. 1993;22:812–818. [PubMed: 7503951]
18. Feng W, Guan Z, Xing D, et al. Avian erythroblastosis virus E26 oncogene homolog-1 (ETS-1) plays a role in renal microvascular pathophysiology in the Dahl salt-sensitive rat. Kidney Int. 2020;97:528–537. [PubMed: 31932071]
19. Miller B, Palygin O, Rufanova VA, et al. p66Shc regulates renal vascular tone in hypertension-induced nephropathy. J Clin Invest. 2016;126:2533–2546. [PubMed: 27270176]
20. Cabral-Pacheco GA, Garza-Veloz I, Castruita-De la Rosa C, et al. The roles of matrix metalloproteinases and their inhibitors in human diseases. Int J Mol Sci. 2020;21:9739. [PubMed: 33419373]
21. Pulido-Olmo H, Garcia-Prieto CF, Alvarez-Llamas G, et al. Role of matrix metalloproteinase-9 in chronic kidney disease: a new biomarker of resistant albuminuria. Clin Sci (Lond). 2016;130:525–538. [PubMed: 26733721]
22. Williams JM, Zhang J, North P, et al. Evaluation of metalloprotease inhibitors on hypertension and diabetic nephropathy. Am J Physiol Renal Physiol. 2011;300:F983–F998. [PubMed: 21228113]
23. Feng W, Chumley P, Prieto MC, et al. Transcription factor avian erythroblastosis virus E26 oncogene homolog-1 is a novel mediator of renal injury in salt-sensitive hypertension. Hypertension. 2015;65:813–820. [PubMed: 25624342]
24. Feng W, Chen B, Xing D, et al. Haploinsufficiency of the transcription factor *Ets-1* is renoprotective in Dahl salt-sensitive rats. J Am Soc Nephrol. 2017;28:3239–3250. [PubMed: 28696249]
25. Oda N, Abe M, Sato Y. ETS-1 converts endothelial cells to the angiogenic phenotype by inducing the expression of matrix metalloproteinases and integrin β3. J Cell Physiol. 1999;178:121–132. [PubMed: 10048576]
26. Zicha J, Dobesova Z, Vokurkova M, et al. Age-dependent salt hypertension in Dahl rats: fifty years of research. Physiol Res. 2012;61(suppl 1):S35–S87. [PubMed: 22827876]
27. Elijovich F, Weinberger MH, Anderson CA, et al. Salt sensitivity of blood pressure: a scientific statement from the American Heart Association. Hypertension. 2016;68:e7–e46. [PubMed: 27443572]
28. Cowley AW Jr, Stoll M, Greene AS, et al. Genetically defined risk of salt sensitivity in an intercross of Brown Norway and Dahl S rats. Physiol Genomics. 2000;2:107–115. [PubMed: 11015589]
29. Moreno C, Dumas P, Kaldunski ML, et al. Genomic map of cardiovascular phenotypes of hypertension in female Dahl S rats. Physiol Genomics. 2003;15:243–257. [PubMed: 14532335]
30. Drueke TB, Devuyst O. Blood pressure measurement in mice: tail-cuff or telemetry? Kidney Int. 2019;96:36. [PubMed: 31229048]
31. Luft FC. Men, mice, and blood pressure: telemetry? Kidney Int. 2019;96: 31–33. [PubMed: 31229046]
32. Feng W, Ying WZ, Aaron KJ, et al. Transforming growth factor-β mediates endothelial dysfunction in rats during high salt intake. Am J Physiol Renal Physiol. 2015;309:F1018–F1025. [PubMed: 26447221]

33. Bondarenko A, Panasiuk O, Stepanenko L, et al. Reduced hyperpolarization of endothelial cells following high dietary Na+: effects of enalapril and tempol. Clin Exp Pharmacol Physiol. 2012;39:608–613. [PubMed: 22540516]
34. Inscho EW, Carmines PK, Navar LG. Juxtamedullary afferent arteriolar responses to P1 and P2 purinergic stimulation. Hypertension. 1991;17:1033–1037. [PubMed: 2045147]
35. Guan Z, Singletary ST, Cook AK, et al. Sphingosine-1-phosphate evokes unique segment-specific vasoconstriction of the renal microvasculature. J Am Soc Nephrol. 2014;25:1774–1785. [PubMed: 24578134]
36. Feng W, Remedies CE, Obi IE, et al. Restoration of afferent arteriolar autoregulatory behavior in ischemia-reperfusion injury in rat kidneys. Am J Physiol Renal Physiol. 2021;320:F429–F441. [PubMed: 33491564]
37. Castro MM, Rizzi E, Figueiredo-Lopes L, et al. Metalloproteinase inhibition ameliorates hypertension and prevents vascular dysfunction and remodeling in renovascular hypertensive rats. Atherosclerosis. 2008;198:320–331. [PubMed: 18054360]
38. Antonio RC, Ceron CS, Rizzi E, et al. Antioxidant effect of doxycycline decreases MMP activity and blood pressure in SHR. Mol Cell Biochem. 2014;386:99–105. [PubMed: 24114660]
39. Ross R The smooth muscle cell. II. Growth of smooth muscle in culture and formation of elastic fibers. J Cell Biol. 1971;50:172–186. [PubMed: 4327464]
40. Xing D, Feng W, Miller AP, et al. Estrogen modulates TNF-α-induced inflammatory responses in rat aortic smooth muscle cells through estrogen receptor-β activation. Am J Physiol Heart Circ Physiol. 2007;292:H2607–H2612. [PubMed: 17237237]
41. Cattaruzza M, Dimigen C, Ehrenreich H, et al. Stretch-induced endothelin B receptor-mediated apoptosis in vascular smooth muscle cells. FASEB J. 2000;14:991–998. [PubMed: 10783154]
42. Garrett MR, Dene H, Rapp JP. Time-course genetic analysis of albuminuria in Dahl salt-sensitive rats on low-salt diet. J Am Soc Nephrol. 2003;14:1175–1187. [PubMed: 12707388]
43. Roman RJ. Abnormal renal hemodynamics and pressure-natriuresis relationship in Dahl salt-sensitive rats. Am J Physiol. 1986;251:F57–F65. [PubMed: 3728685]
44. Takenaka T, Forster H, De Micheli A, et al. Impaired myogenic responsiveness of renal microvessels in Dahl salt-sensitive rats. Circ Res. 1992;71:471–480. [PubMed: 1628401]
45. Byon CH, Javed A, Dai Q, et al. Oxidative stress induces vascular calcification through modulation of the osteogenic transcription factor Runx2 by AKT signaling. J Biol Chem. 2008;283:15319–15327. [PubMed: 18378684]
46. Sun Y, Byon CH, Yuan K, et al. Smooth muscle cell-specific Runx2 deficiency inhibits vascular calcification. Circ Res. 2012;111:543–552. [PubMed: 22773442]
47. Raaz U, Schellinger IN, Chernogubova E, et al. Transcription factor Runx2 promotes aortic fibrosis and stiffness in type 2 diabetes mellitus. Circ Res. 2015;117:513–524. [PubMed: 26208651]
48. Lin ME, Chen TM, Wallingford MC, et al. Runx2 deletion in smooth muscle cells inhibits vascular osteochondrogenesis and calcification but not atherosclerotic lesion formation. Cardiovasc Res. 2016;112:606–616. [PubMed: 27671804]
49. Ducy P, Zhang R, Geoffroy V, et al. Osf2/Cbfa1: a transcriptional activator of osteoblast differentiation. Cell. 1997;89:747–754. [PubMed: 9182762]
50. Lian JB, Javed A, Zaidi SK, et al. Regulatory controls for osteoblast growth and differentiation: role of Runx/Cbfa/AML factors. Crit Rev Eukaryot Gene Expr. 2004;14:1–41. [PubMed: 15104525]
51. Bidani AK, Griffin KA, Williamson G, et al. Protective importance of the myogenic response in the renal circulation. Hypertension. 2009;54:393–398. [PubMed: 19546375]
52. Loutzenhiser R, Griffin K, Williamson G, et al. Renal autoregulation: new perspectives regarding the protective and regulatory roles of the underlying mechanisms. Am J Physiol Regul Integr Comp Physiol. 2006;290:R1153–R1167. [PubMed: 16603656]
53. Carlstrom M, Wilcox CS, Arendshorst WJ. Renal autoregulation in health and disease. Physiol Rev. 2015;95:405–511. [PubMed: 25834230]
54. Burke M, Pabbidi MR, Farley J, et al. Molecular mechanisms of renal blood flow autoregulation. Curr Vasc Pharmacol. 2014;12:845–858. [PubMed: 24066938]

55. Griffin KA. Hypertensive kidney injury and the progression of chronic kidney disease. Hypertension. 2017;70:687–694. [PubMed: 28760941]
56. Kotchen TA, Piering AW, Cowley AW, et al. Glomerular hyperfiltration in hypertensive African Americans. Hypertension. 2000;35:822–826. [PubMed: 10720601]
57. Sterzel RB, Luft FC, Gao Y, et al. Renal disease and the development of hypertension in salt-sensitive Dahl rats. Kidney Int. 1988;33:1119–1129. [PubMed: 3404812]
58. Karlsen FM, Andersen CB, Leyssac PP, et al. Dynamic autoregulation and renal injury in Dahl rats. Hypertension. 1997;30:975–983. [PubMed: 9336403]
59. Moore LC. Interaction of tubuloglomerular feedback and proximal nephron reabsorption in autoregulation. Kidney Int Suppl. 1982;12:S173–S178. [PubMed: 6957673]
60. Ahmed A, Rich MW, Sanders PW, et al. Chronic kidney disease associated mortality in diastolic versus systolic heart failure: a propensity matched study. Am J Cardiol. 2007;99:393–398. [PubMed: 17261405]
61. Schnermann J, Briggs J, Wright FS. Feedback-mediated reduction of glomerular filtration rate during infusion of hypertonic saline. Kidney Int. 1981;20:462–468. [PubMed: 7311307]
62. Karlsen FM, Leyssac PP, Holstein-Rathlou NH. Tubuloglomerular feedback in Dahl rats. Am J Physiol. 1998;274:R1561–R1569. [PubMed: 9608009]
63. Takenaka T, Harrison-Bernard LM, Inscho EW, et al. Autoregulation of afferent arteriolar blood flow in juxtamedullary nephrons. Am J Physiol. 1994;267:F879–F887. [PubMed: 7977792]
64. Guan Z, Wang F, Cui X, et al. Mechanisms of sphingosine-1-phosphate-mediated vasoconstriction of rat afferent arterioles. Acta Physiol (Oxf). 2018;222(2).
65. Sato Y, Wharram BL, Lee SK, et al. Urine podocyte mRNAs mark progression of renal disease. J Am Soc Nephrol. 2009;20:1041–1052. [PubMed: 19389856]
66. Wickman L, Afshinnia F, Wang SQ, et al. Urine podocyte mRNAs, proteinuria, and progression in human glomerular diseases. J Am Soc Nephrol. 2013;24:2081–2095. [PubMed: 24052633]
67. Kriz W, Lemley KV. A potential role for mechanical forces in the detachment of podocytes and the progression of CKD. J Am Soc Nephrol. 2015;26:258–269. [PubMed: 25060060]
68. Wozniak J, Floege J, Ostendorf T, et al. Key metalloproteinase-mediated pathways in the kidney. Nat Rev Nephrol. 2021;17:513–527. [PubMed: 33879883]
69. Bengatta S, Arnould C, Letavernier E, et al. MMP9 and SCF protect from apoptosis in acute kidney injury. J Am Soc Nephrol. 2009;20: 787–797. [PubMed: 19329763]
70. Lee SY, Horbelt M, Mang HE, et al. MMP-9 gene deletion mitigates microvascular loss in a model of ischemic acute kidney injury. Am J Physiol Renal Physiol. 2011;301:F101–F109. [PubMed: 21454251]
71. Catania JM, Chen G, Parrish AR. Role of matrix metalloproteinases in renal pathophysiologies. Am J Physiol Renal Physiol. 2007;292:F905–F911. [PubMed: 17190907]
72. Yu Q, Stamenkovic I. Cell surface-localized matrix metalloproteinase-9 proteolytically activates TGF-β and promotes tumor invasion and angiogenesis. Genes Dev. 2000;14:163–176. [PubMed: 10652271]
73. Sharma K, Cook A, Smith M, et al. TGF-β impairs renal autoregulation via generation of ROS. Am J Physiol Renal Physiol. 2005;288:F1069–F1077. [PubMed: 15644487]
74. Chen Y, Zhao X, Wu H. Arterial stiffness: a focus on vascular calcification and its link to bone mineralization. Arterioscler Thromb Vasc Biol. 2020;40:1078–1093. [PubMed: 32237904]
75. Ebel ME, Kansas GS. Functions of Smad transcription factors in TGF-β1-induced selectin ligand expression on murine CD4 Th cells. J Immunol. 2016;197:2627–2634. [PubMed: 27543612]
76. Baxter BT, Matsumura J, Curci JA, et al. Effect of doxycycline on aneurysm growth among patients with small infrarenal abdominal aortic aneurysms: a randomized clinical trial. JAMA. 2020;323:2029–2038. [PubMed: 32453369]

Translational Statement

Hypertensive nephropathy involves kidney dysfunction and microvascular pathology. Using salt-sensitive (SS) rats, the present studies discovered a matrix metalloproteinase-9 (MMP-9)–dependent, hypertension-induced osteogenic phenotypic switch by kidney microvascular smooth muscle cells, with concomitant dysregulation of microvascular function. Kidney dysfunction and podocyte injury followed these changes in SS but not in SS rats that lack *Mmp9*. The observations provide new opportunities for exploration of early diagnosis of impaired kidney autoregulation in hypertension and for development of novel therapeutic strategies that protect against this common mediator of chronic kidney disease.

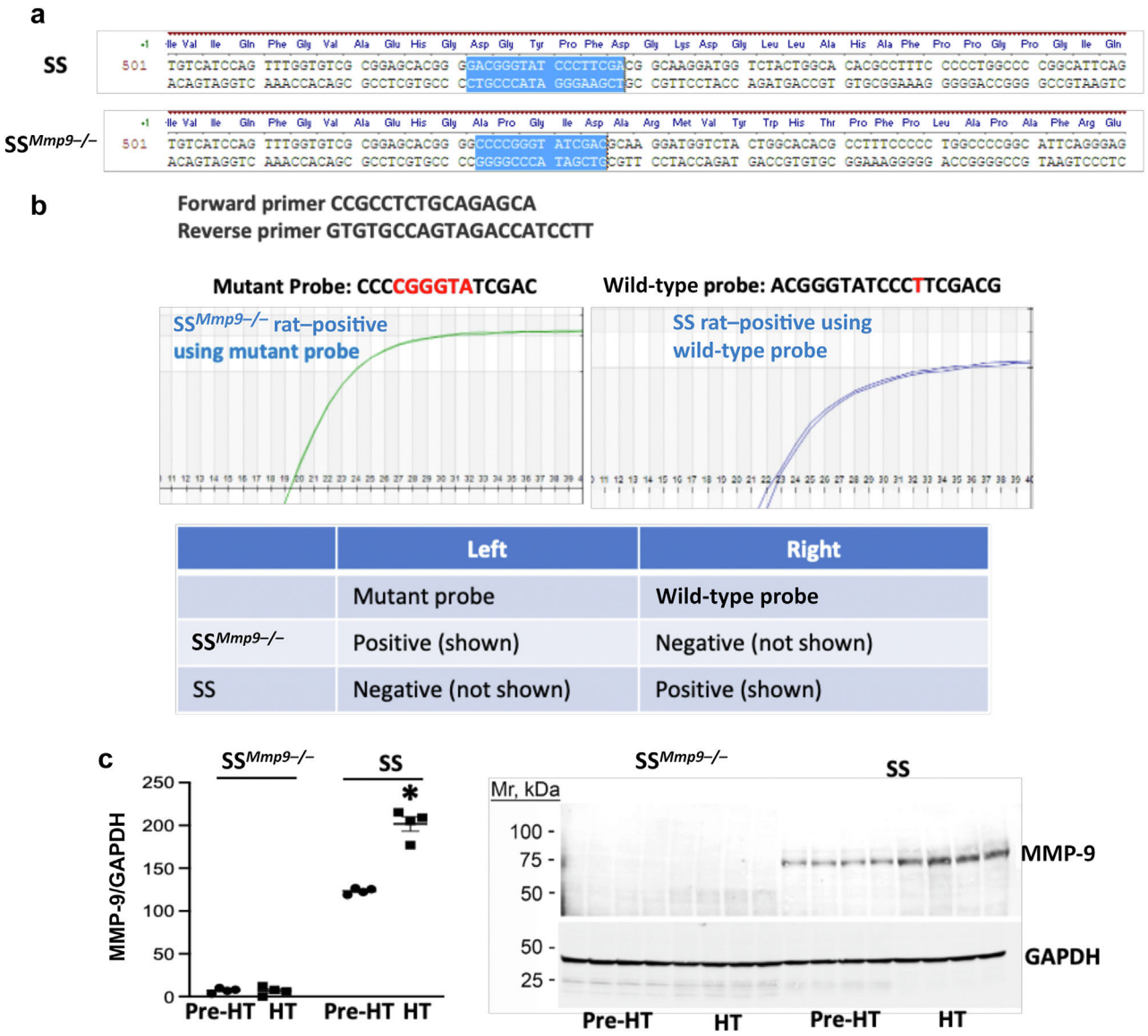

Figure 1|. Development of hypertension increases matrix metalloproteinase-9 (MMP-9) expression in the kidney cortex.

(a) The genomic sequence of *Mmp9* was altered using the CRISPR/Cas9 system, which deleted 1-bp (t) and inserted 5-bp (cgggta) in exon 4, producing a frameshift mutation. **(b)** Genotypes of homozygous salt-sensitive (SS) rats that lack *Mmp9* (SS$^{Mmp9-/-}$ rats) and littermate control SS rats were confirmed using TaqMan probe real-time polymerase chain reaction (PCR; Transnetyx). Following PCR using the primers shown, the amplified product was probed with either the mutant (*left panel*) or the wild-type (*right panel*) probe. *Left panel*: Amplicon from DNA of an SS$^{Mmp9-/-}$ rat that was positive using the mutant probe (cycle threshold about 19, sample in duplicate). Amplicons from SS rats generated no signal using the mutant probe (not shown). *Right panel*: Amplicon from DNA of an SS rat that was positive using the wild-type probe (cycle threshold about 22, sample in duplicate); no signal from SS$^{Mmp9-/-}$ rats was observed using the wild-type probe (not shown). **(c)** Littermate SS control and SS$^{Mmp9-/-}$ rats maintained on either the 0.3% NaCl diet (labeled Pre-HT) or the

4.0% NaCl diet (labeled HT) for 7 days were studied. Western analysis at day 7 confirmed the absence of MMP-9 in SS$^{Mmp9-/-}$ rats on both diets and also demonstrated increased expression of MMP-9 relative to glyceraldehyde-3-phosphate dehydrogenase (GAPDH) in the kidney cortex in HT SS compared with Pre-HT SS rats. *$P < 0.05$, Pre-HT SS rats versus HT SS rats. Data were expressed as mean ± SEM and were analyzed using 2-way analysis of variance and Tukey post hoc test. Mr, relative molecular mass.

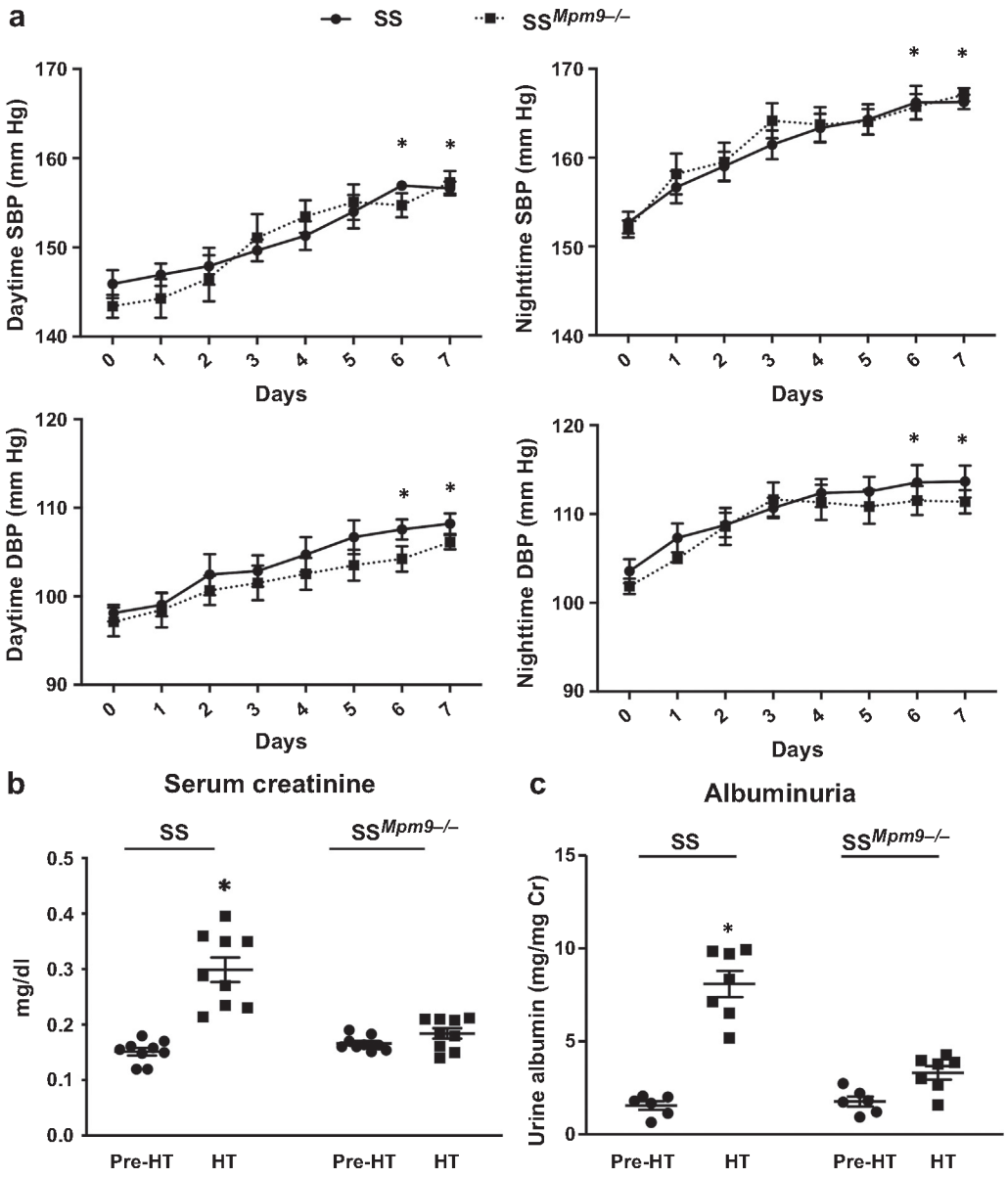

Figure 2|. Kidney injury developed in hypertensive salt-sensitive (SS) rats but was abrogated in SS rats that lack matrix metalloproteinase-9 (*Mmp9*) (SS$^{Mmp9-/-}$ rats) despite a similar increase in telemetry-monitored blood pressure.

(a) At baseline, telemetry-monitored mean systolic blood pressure (SBP) and diastolic blood pressure (DBP) did not differ between SS (solid line) and SS$^{Mmp9-/-}$ (dashed line) rats. One week of high salt intake increased SBP and DBP in both SS and SS$^{Mmp9-/-}$ rats. $n = 6$ rats in each group. *$P < 0.05$, SS rats fed a control diet containing 0.3% NaCl (Pre-HT SS rats) versus SS rats fed a 4% NaCl diet for 1 week to induce hypertension (HT SS rats), SS$^{Mmp9-/-}$ rats fed a control diet containing 0.3% NaCl (Pre-HT SS$^{Mmp9-/-}$ rats) versus SS$^{Mmp9-/-}$ rats fed a 4% NaCl diet for 1 week to induce hypertension (HT SS$^{Mmp9-/-}$ rats). The strain effect (SS or SS$^{Mmp9-/-}$) and the increase in SBP and DBP did not differ between SS$^{Mmp9-/-}$ and SS rats. $n = 6$. $P > 0.05$, HT SS rats versus HT SS$^{Mmp9-/-}$ rats. **(b)** Hypertension increased mean serum creatinine concentration of the HT SS group but not the

HT SS$^{Mmp9-/-}$ group. $n = 9$ rats in each group. *$P < 0.05$ versus the other 3 groups. (c) After 1 week of high salt intake, HT SS rats also showed a significant increase in mean urinary albumin excretion as compared with the other 3 groups of rats. $n = 6$ to 7. *$P < 0.05$. Data were expressed as mean ± SEM. Blood pressure data were analyzed using 2-way analysis of variance for repeated measures and Dunnett post hoc test. Serum creatinine and albuminuria data were analyzed using 2-way analysis of variance and Tukey *post hoc* test.

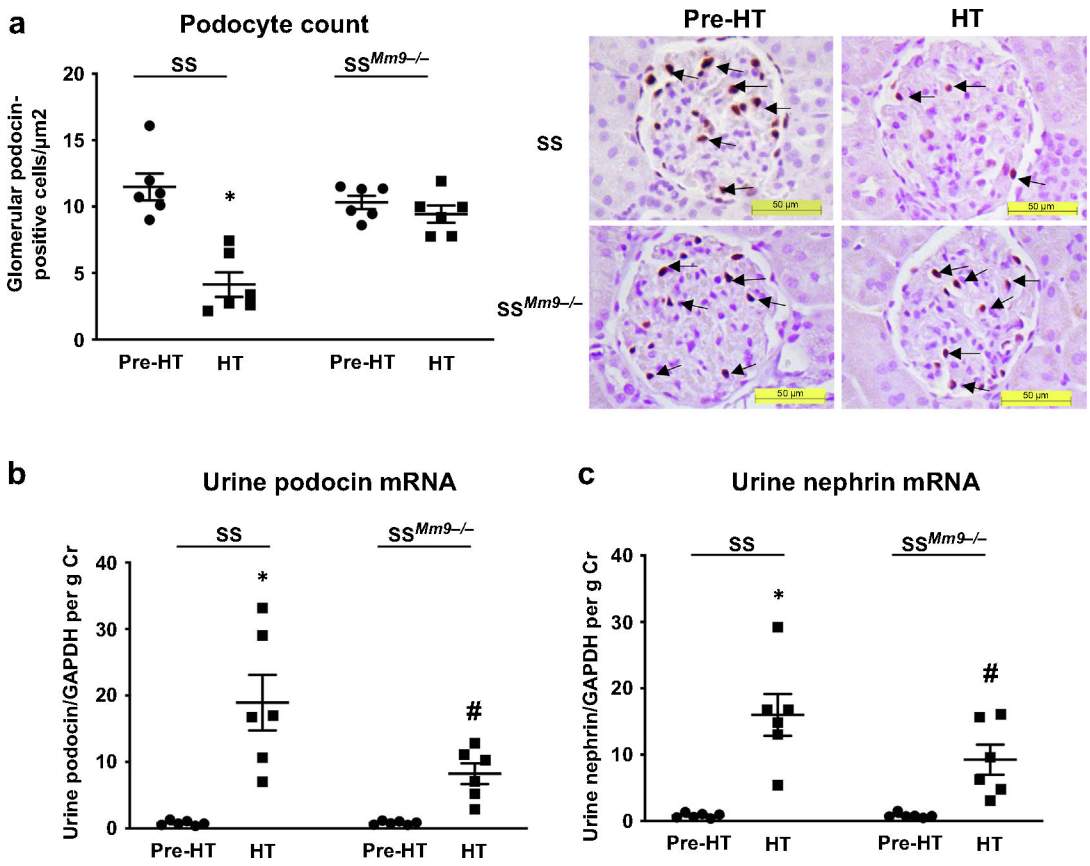

Figure 3|. Podocyte injury developed with hypertension in salt-sensitive (SS) rats, whereas hypertensive SS rats that lack matrix metalloproteinase-9 (*Mmp9*) (SS$^{Mmp9-/-}$ rats) were protected.

(a) Blind analysis of photomicrographs of immunohistochemical (IHC) staining using Wilms' tumor 1 (WT1) protein antibody to outline the nuclei of podocytes (arrows) showed that hypertension decreased WT1-positive cells in SS but not in SS$^{Mmp9-/-}$ rats. $n = 6$ rats in each group. SS rats fed a 4% NaCl diet for 1 week to induce hypertension (HT SS rats) versus SS$^{Mmp9-/-}$ rats fed a 4% NaCl diet for 1 week to induce hypertension (HT SS$^{Mmp9-/-}$ rats), 3.66 0.97 versus 9.29 0.91. *$P < 0.05$. Representative photomicrographs of IHC staining are shown. (**b,c**) HT SS rats showed a significant increase in urinary podocin and nephrin mRNA excretion as compared with Pre-HT SS rats that are significantly reduced in SS$^{Mmp9-/-}$ rats. $n = 6$. *$P < 0.05$ versus Pre-HT SS rats, #$P < 0.05$ versus HT SS rats. Data were expressed as mean ± SEM and were analyzed using 2-way analysis of variance and Tukey *post hoc* test.. To optimize viewing of this image, please see the online version of this article at www.kidney-international.org.

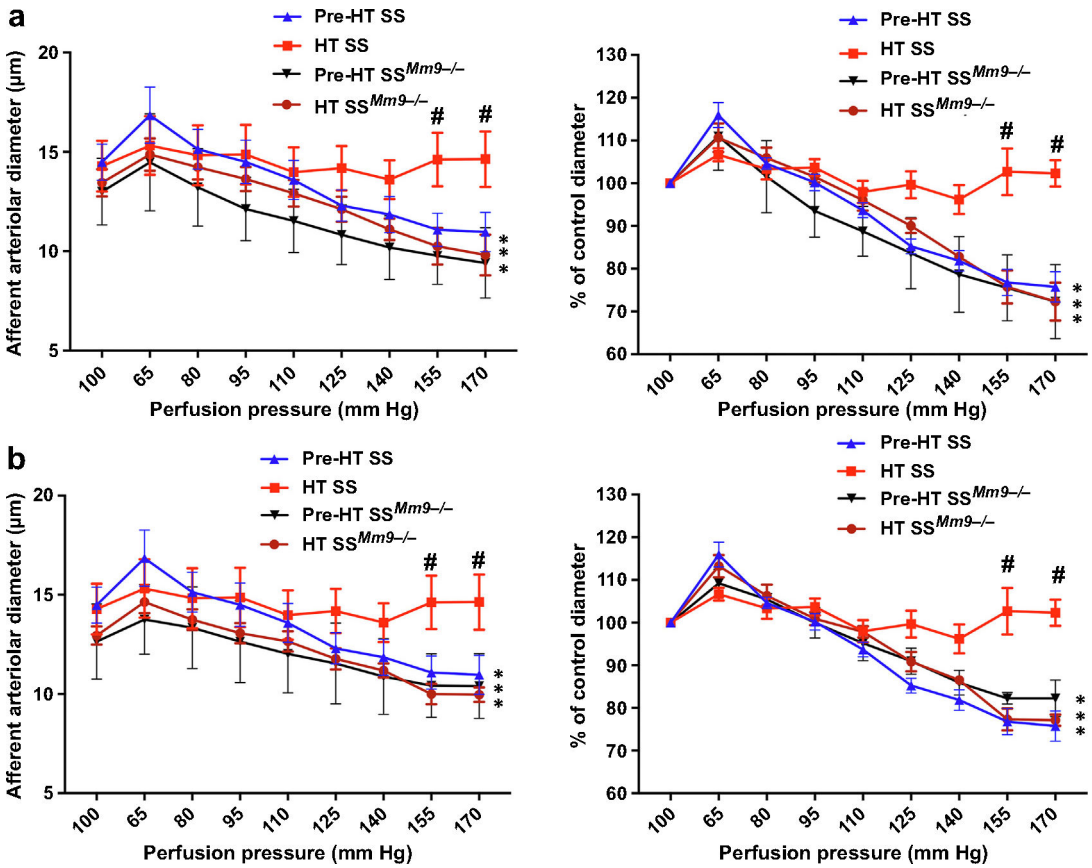

Figure 4|. Inhibition of matrix metalloproteinase-9 (MMP-9) improved kidney microvasculature autoregulation in salt-sensitive (SS) rats fed a 4% NaCl diet for 1 week to induce hypertension (HT SS rats).

Afferent arteriolar autoregulation was assessed using an *in vitro* blood-perfused juxtamedullary nephron preparation. *Left panels*: Changes in mean diameters of afferent arterioles in response to alteration of renal perfusion pressure *Right panels*: Data normalized as a percentage of the control diameter at 100 mm Hg. **(a)** Afferent arteriolar autoregulation was assessed in SS rats and SS rats that lack *Mmp9* (SS$^{Mmp9-/-}$ rats) after 7 days maintained on either a 0.3% salt diet (Pre-HT and Pre-HT SS$^{Mmp9-/-}$ rats, respectively) or a 4.0% salt diet (HT SS and HT SS$^{Mmp9-/-}$). Both strain effect (SS or SS$^{Mmp9-/-}$) and perfusion pressure effect are significant ($P < 0.05$), and the curves are different. $P < 0.05$. **(b)** In separate experiments, afferent arteriolar autoregulation was determined in SS rats treated with either vehicle or doxycycline (Dox) fed the low-salt diet (Pre-HT SS and Pre-HT SS + Dox) or the high-salt diet (HT SS and HT SS + Dox). Treatment effect (Dox) and perfusion pressure effect are significant ($P < 0.05$), and the curves are different. $P < 0.05$. In both studies, loss of autoregulation produced by the development of hypertension in SS rats was prevented by either MMP-9 knockout (KO) or treatment with Dox. $n = 5$ to 7. *$P < 0.05$ versus control diameter in the same group, #$P < 0.05$ versus Pre-HT SS kidneys at the same perfusion pressure. Data were expressed as mean ± SEM and were analyzed using 2-way analysis of variance for repeated measures. *Post hoc* test was performed using a Dunnett multiple comparisons test.

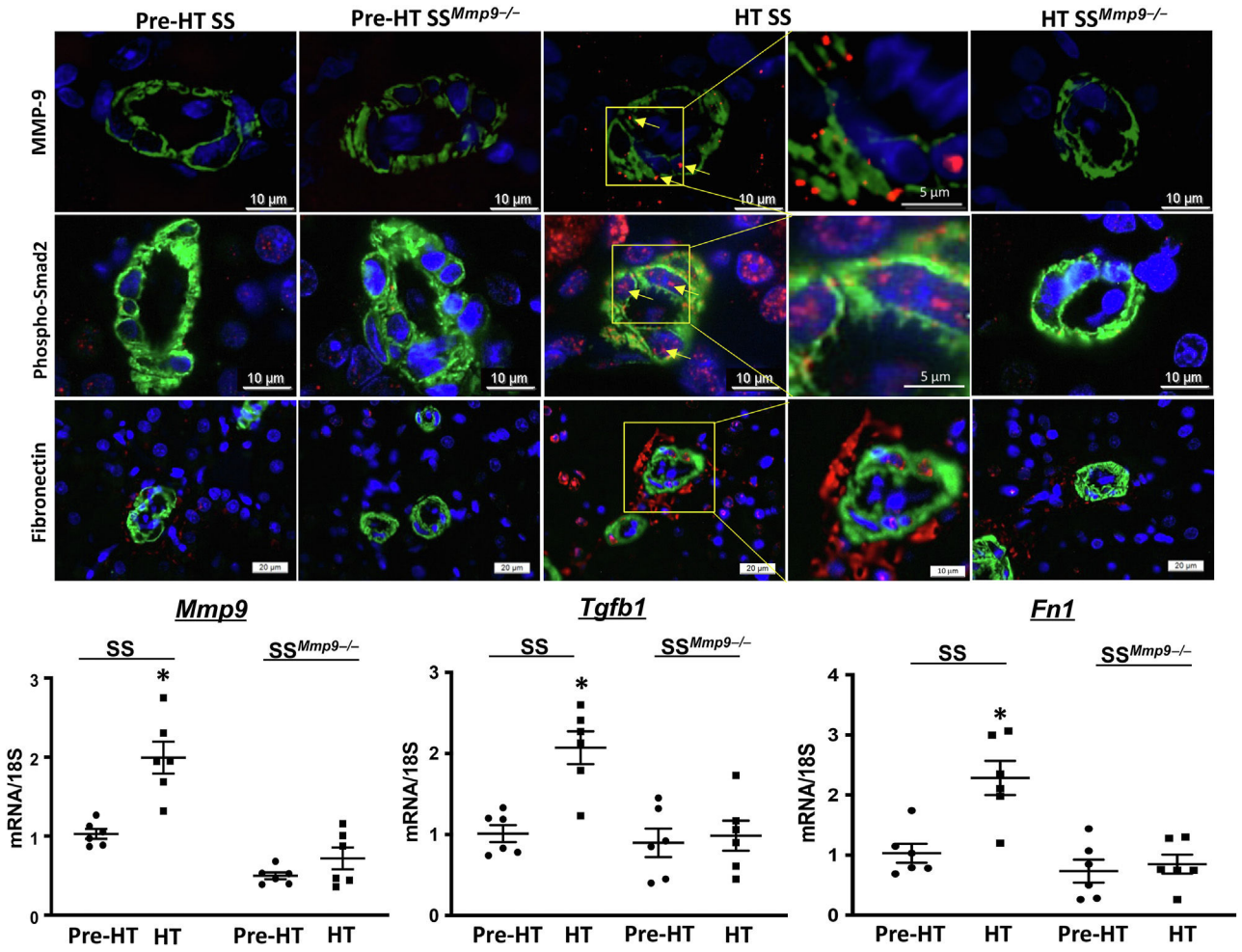

Figure 5|. Matrix metalloproteinase-9 (MMP-9) and the transforming growth factor-β (TGF-β) pathway are activated in kidney microvessels of hypertensive salt-sensitive (SS) rats but not of hypertensive SS rats that lack *Mmp9* (SS$^{Mmp9-/-}$ rats).

Top panels: Immunofluorescence microscopy used α-smooth muscle actin antibody (green) to outline kidney arterioles, which were 1 to 2 smooth muscle cells thick and <50 μm in diameter. Using antibodies to MMP-9, phosphorylated Smad2 (phospho-Smad2), and fibronectin (red), MMP-9, active Smad2, and fibrinogen were identified (yellow arrows) in the smooth muscle cell layer of kidney microvessels of SS rats fed a 4% NaCl diet for 1 week to induce hypertension (HT SS rats) but not of SS rats fed a control diet containing 0.3% NaCl (Pre-HT SS rats), SS$^{Mmp9-/-}$ rats fed a control diet containing 0.3% NaCl (Pre-HT SS$^{Mmp9-/-}$ rats), and SS rats fed a 4% NaCl diet for 1 week to induce hypertension (HT SS$^{Mmp9-/-}$ rats). *Bottom panels*: Experiments using total RNA isolated from kidney microvessels showed low basal mRNA levels of *Mmp9*, *Tgfb1*, and *Fn1* in Pre-HT SS and Pre-HT SS$^{Mmp9-/-}$ rats. The amount of these mRNAs increased specifically in the group of HT SS rats. $n = 6$ animals in each group. *$P < 0.05$ versus Pre-HT SS, Pre-HT SS$^{Mmp9-/-}$, and HT SS$^{Mmp9-/-}$ groups. To optimize viewing of this image, please see the online version of this article at www.kidney-international.org.

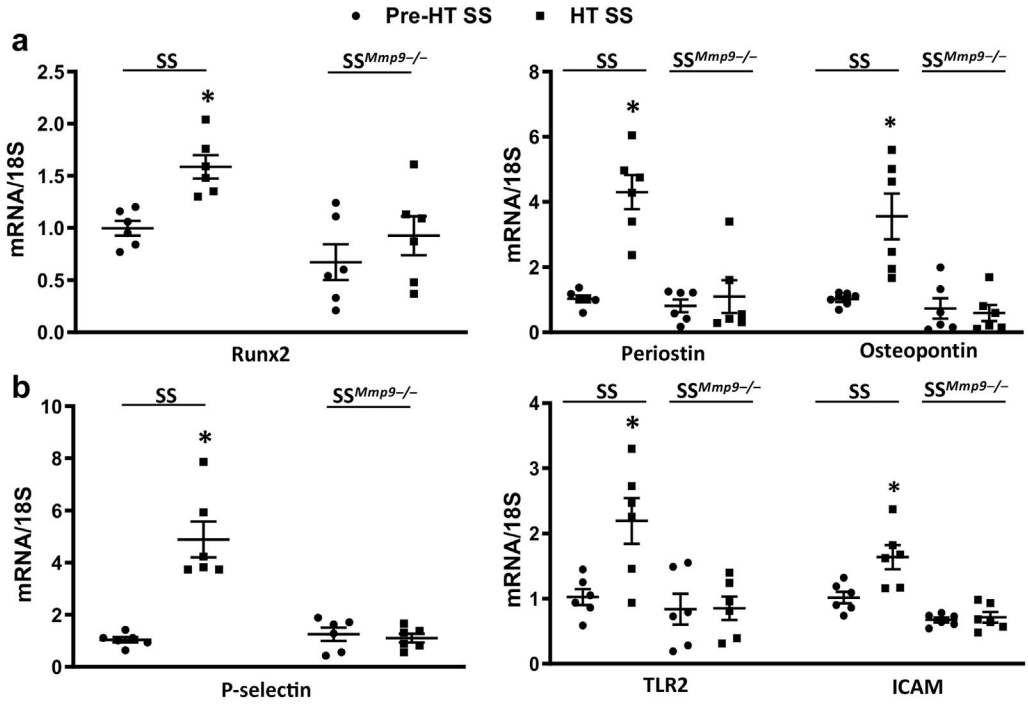

Figure 6|. Microdissected arterioles of salt-sensitive (SS) rats fed a 4% NaCl diet for 1 week to induce hypertension (HT SS rats) but not of SS rats that lack matrix metalloproteinase-9 (*Mmp9*) (SS$^{Mmp9-/-}$ rats) demonstrated increased mean steady-state relative mRNA levels of pro-osteogenic and pro-inflammatory molecules.

(a) Kidney microvascular mRNA expression of pro-osteogenic molecules Runt-related transcription factor 2 (Runx2), periostin, and osteopontin increased 1.5-, 4.2-, and 3.3-fold, respectively, in HT SS rats and were greater than corresponding levels in microvessels of SS rats fed a control diet containing 0.3% NaCl (Pre-HT SS rats), SS$^{Mmp9-/-}$ rats fed a control diet containing 0.3% NaCl (Pre-HT SS$^{Mmp9-/-}$ rats), and SS$^{Mmp9-/-}$ rats fed a 4% NaCl diet for 1 week to induce hypertension (HT SS$^{Mmp9-/-}$ rats). $n = 6$ animals in each group. $^{*}P < 0.05$ versus Pre-HT SS, Pre-HT SS$^{Mmp9-/-}$, and HT SS$^{Mmp9-/-}$ groups. (b) Kidney microvascular mRNA expression of inflammatory mediators P-selectin, Toll-like receptor 2 (TLR2), and intercellular adhesion molecule (ICAM) increased 5.0-, 2.2-, and 1.7-fold, respectively, in HT SS rats and were greater than levels of expression observed in microvessels of Pre-HT SS, Pre-HT SS$^{Mmp9-/-}$, and HT SS$^{Mmp9-/-}$ rats. $n = 6$ animals in each group. $^{*}P < 0.05$ versus Pre-HT SS, Pre-HT SS$^{Mmp9-/-}$, and HT SS$^{Mmp9-/-}$ groups. Data were expressed as mean SEM and were analyzed using 2-way analysis of variance and Tukey post hoc test.

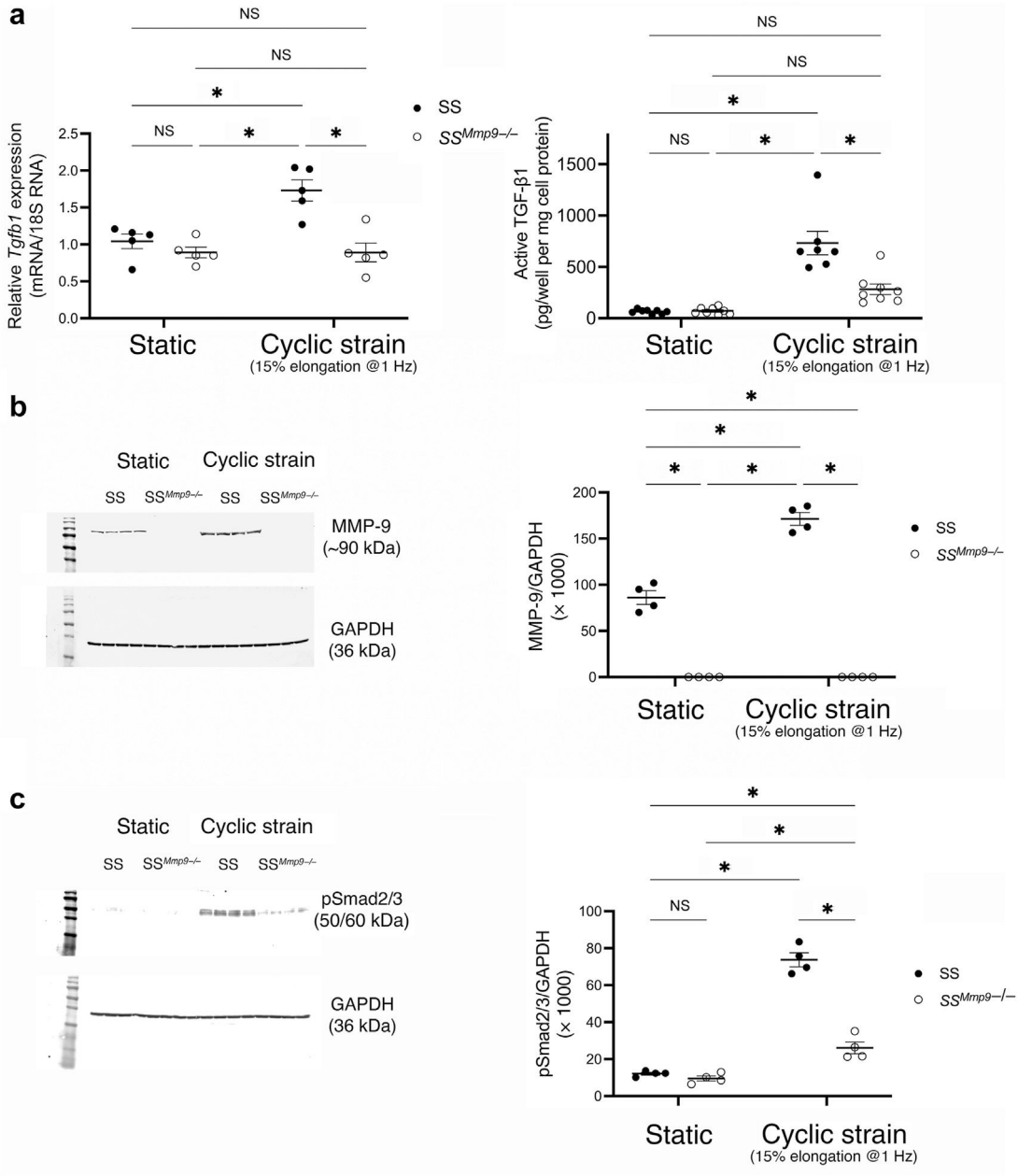

Figure 7|. Cyclic strain activates the canonical transforming growth factor-β (TGF-β) signaling pathway in vascular smooth muscle cells (VSMCs) from salt-sensitive (SS) rats but not in VSMCs from SS rats that lack matrix metalloproteinase-9 (*Mmp9*) (SS$^{Mmp9-/-}$ rats).

(a) Top *left panel*: Cyclic strain (15% elongation at 1 Hz) increased relative expression of *Tgfb1* specifically in VSMCs from SS rats. $n = 5$ samples in each group. *P < 0.05. Data analyzed using 2-way analysis of variance (ANOVA) and Tukey *post hoc test*. Top right panel: Induction of cyclic strain increased levels of active TGF-β1 in the medium of VSMCs from SS rats. $n = 6$ samples in each group. *$P < 0.05$. Data analyzed using 2-way ANOVA and Tukey *post hoc test*. **(b)** Compared to wild-type cells under static conditions, cyclic strain (15% elongation at 1 Hz) increased relative expression of *Mmp9*; mRNA was not present in samples from *Mmp9* knockout rats (right panel). $n = 4$ samples in each group. *P

< 0.05. Data analyzed using 2-way ANOVA and Tukey *post hoc test*. **(c)** Western analysis showed increased phosphorylated Smad2/3 (pSmad2/3) in VSMCs from SS rats exposed to cyclic strain. $n = 4$ samples in each group. $*P < 0.05$. Data analyzed using 2-way analysis of variance and Tukey *post hoc* test. GAPDH, glyceraldehyde-3-phosphate dehydrogenase; NS, not significant.

Table 1|

Primers used in real-time polymerase chain reaction analyses

Gene	Forward primer	Reverse primer
Mmp9	GAATCACGGAGGAAGCCAAT	GTGTACACCCACATTTTGCG
Nphs2 (podocin)	GCAGTCTAGCTCATGTGTCC	CTGAGTCCAAGGCAACCTTT
Nphs1 (nephrin)	CTGTGGACATAGTCTGCACC	CTTTCTCCATGTCGTCCAGG
Tgfb1	CTACTGCTTCAGCTCCACAGAGA	ACCTTGGGCTTGCGACC
Fn1 (fibronectin)	GCCTTCAACTTCTCCTGTGA	GTTGCAAACCTTCAATGGTC
Runx2	TGACCTTTGTCCCAATGTGG	TTTGCTACTGGGTGGGTTTC
Spp1 (osteopontin)	AGGAGTTTCCCTGTTTCTG	GTCTTCCCGTTGCTGTC
Postn (periostin)	CATAGACGGGGTTCCTGTTG	TGCAAGAATTTCTGCAGGGT
Selp (P-selectin)	AATGAAATCGCTCACCTC	TTATTGGGCTCGTTGTCT
TLR2	GCTCCTGTGAACTCCTGTCC	GACACTCCAAGACTGAGGGC
ICAM	CAAACGGGAGATGAATGG	TGGCGGTAATAGGTGTAAAT
GAPDH	ATTCTTCCACCTTTGATGC	TGGTCCAGGGTTTCTTACT
18S	ATTTGACTCAACACGGGAAA	TCGCTCCACCAACTAAGAAC